

1 Impacts of the seasonal distribution of rainfall on vegetation productivity 2 across the Sahel

3 Wenmin Zhang^{a,b}, Martin Brandt^b, Xiaoye Tong^b, Qingjiu Tian^{a*□}, Rasmus Fensholt^b

4 ^a *International Institute for Earth System Sciences, Nanjing University, 210023 Nanjing, China*

5 ^b *Department of Geosciences and Natural Resource Management, University of Copenhagen, 1350 Copenhagen,
6 Denmark*

7

8 **Abstract** Climate change in drylands has caused alterations in the seasonal distribution of rainfall including increased heavy
9 rainfall events, longer dry spells, and a shifted timing of the wet season. Yet, the aboveground net primary productivity
10 (ANPP) in drylands is usually explained by annual rainfall sums, disregarding the influence of the seasonal distribution of
11 rainfall. This study tested the importance of rainfall metrics in the wet season (onset and cessation of the wet season, number
12 of rainy days, rainfall intensity, number of consecutive dry days and heavy rainfall events) on growing season ANPP. We
13 focused on the Sahel and north-Sudanian region (100-800 mm yr⁻¹) and applied daily satellite based rainfall estimates
14 (CHIRPS v2.0) and growing season integrated NDVI (MODIS) as a proxy for ANPP over the study period 2001-2015.
15 Growing season ANPP in the arid zone (100-300 mm yr⁻¹) was found to be rather insensitive to variations in the seasonal
16 rainfall metrics, whereas vegetation in the semi-arid zone (300-700 mm yr⁻¹) was significantly impacted by most metrics,
17 especially by the number of rainy days and timing (onset and cessation) of the wet season. We analyzed critical breakpoints
18 for all metrics to test if vegetation response to changes in a given rainfall metric surpasses a threshold beyond which
19 vegetation functioning is significantly altered. It was shown that growing season ANPP was particularly negatively impacted
20 after >14 consecutive dry days and that a rainfall intensity of ~13 mm day⁻¹ was detected for optimum growing season ANPP.
21 We conclude that number of rainy days and the timing of the wet season are seasonal rainfall metrics being decisive for

* Corresponding author at: Kunshan Building Xianlin avenue,163#, Nanjing, China

E-mail address: tianqj@nju.edu.cn (Q.Tian).

22 favorable vegetation growth in semi-arid Sahel which needs to be considered when modelling primary productivity from
23 rainfall in the dryland's of Sahel and elsewhere.

24 **Keywords:** Drylands, Seasonal rainfall metrics, Aboveground net primary production, Remote sensing

25

26 **1 Introduction**

27 Livihoods in most drylands depend heavily on aboveground net primary production (ANPP) in the form of
28 rain-fed crops and fodder for livestock (Abdi et al., 2014; Leisinger and Schmitt, 1995). Annual ANPP thus plays
29 a decisive role in the context of livelihood strategies, food security and people's general wellbeing. ANPP in
30 drylands is primarily controlled by water availability with annual rainfall typically being limited to a short and
31 erratic wet season which can be highly variable in time and space. The current study focuses on the sub-Saharan
32 Sahel zone which is one of the largest dryland areas in the world. The Sahel has been referred to as the region
33 showing the largest rainfall anomalies worldwide during the last century (Nicholson, 2000). Throughout the
34 centuries, the Sahelian population has adapted to this high rainfall variability and the associated great inter-annual
35 differences in available ANPP are balanced for example by a temporary abandonment of agriculture or seasonal
36 livestock migration (Romankiewicz et al., 2016). However, 21st century climate change is predicted to threaten
37 established coping strategies; not only by increasing inter-annual variability of rainfall regimes as a whole (Field,
38 2012; Kharin et al., 2007), but also by an increasingly unpredictable seasonality and an altered number of heavy
39 rainfall and drought events (Fischer et al., 2013; Smith, 2011; Taylor et al., 2017). Improved knowledge on the
40 vegetation response to the seasonal variability of rainfall is thus crucial to better interpret the consequences of
41 climate predictions of an altered global hydrological cycle and to implement appropriate adaptation measures to
42 climate change and food security in arid and semi-arid lands like the Sahel.

43 While it is well known that the productivity of dryland vegetation is highly prone to variations in the
44 availability of water resources at the annual scale (Fensholt et al., 2013; Fensholt and Kjeld, 2011; Herrmann et

45 al., 2005; Huber et al., 2011), there is a current lack of understanding how the seasonal distribution of rainfall
46 impacts on growing season ANPP (Rishmawi et al., 2016). Several studies have demonstrated the vegetation
47 sensitivity to the timing and magnitude of rainfall events based on individual plot data and model estimates
48 (Bates et al., 2006; Fay et al., 2000; Guan et al., 2014; Thomey et al., 2011), but the impact of specific rainfall
49 metrics (such as wet season length/timing, number of rainy days, rainfall intensity, number of consecutive dry
50 days and extreme events) on dryland vegetation productivity has rarely been studied in spatially distributed
51 manner, potentially including different biotic and abiotic controls. A few studies show that there is a strong
52 dependency of Sahelian vegetation growth on the timing of the wet season (Diouf et al., 2016) and the frequency
53 and distribution of dry spells (Proud and Rasmussen, 2011), but currently no regional scale study have
54 systematically analyzed the importance of a variety rainfall metrics on vegetation growth as a function of mean
55 annual rainfall. Further, there is evidence showing that not only a shift in the timing of the wet season but also
56 increasing extreme events occur in Sahel (Panthou et al., 2014; Sanogo et al., 2015; Taylor et al., 2017; Zhang et
57 al., 2017), suggesting the need for a comprehensive understanding on how rainfall seasonality impacts on
58 vegetation production.

59 The assessment of rainfall metrics capturing the seasonal variability and the associated impact on growing
60 season ANPP requires daily rainfall records and a robust methodology being able to extract the timing (onset and
61 cessation) and duration of the wet season (Dunning et al., 2016; Liebmann et al., 2012). The availability and
62 quality of such data, and uncertainties in methods to extract the rainfall seasonality have complicated regionally
63 scaled studies on this topic (Fitzpatrick et al., 2015). However, a new generation of high spatial resolution
64 satellite based daily rainfall estimates blended with station data has recently opened up the possibility to fill the
65 gap between plot and model based studies. Here our study aims at applying daily rainfall estimates to analyze and
66 understand the impact of seasonal rainfall metrics on vegetation productivity for the entire Sahel.

67

68 **2 Materials and methods**

69 An empirical analysis was conducted based on gridded information of rainfall metrics based on daily
70 satellite estimates and seasonally integrated NDVI (hereafter \sum NDVI) as a proxy for the growing season ANPP.
71 The period of analysis covers 2001-2015 which allows for a per-pixel analysis including state of the art Earth
72 observation datasets of both Climate Hazards Group InfraRed Precipitation with Station (CHIRPS v2.0) and
73 Moderate Resolution Imaging Spectroradiometer (MODIS) vegetation. The rainfall metrics include: number of
74 rainy days, daily intensity, heavy rainfall events, number of consecutive dry days and seasonal rainfall amount
75 which were analyzed as explanatory variables for the observed spatial variability in seasonal vegetation
76 productivity along the gradient of mean seasonal rainfall.

77

78 **2.1 Study area**

79 The Sahelian zone covers arid and semi-arid biomes and is one of the world's largest dryland areas
80 bordering the Sahara Desert to the north (Fig. 1). The delineation of the Sahel is often done by using average
81 annual rainfall isohyets, with the northern boundary at 100 mm yr⁻¹ and the southern boundary defined by 700
82 mm yr⁻¹ (Lebel and Ali, 2009). For this study we expanded the southern limit towards the Sudanian zone until
83 800 mm yr⁻¹ to include also the zone where rainfall as the primary climatic forcing variable on vegetation
84 productivity is expected to level off (Fensholt et al., 2013; Huber et al., 2011; Kaspersen et al., 2011). The Sahel
85 is characterized by a unimodal rainfall regime and the landscape is generally flat and consists of large plains
86 interspersed with sand dunes and rocky formations. The large stretches of plains are mainly used for grazing and
87 subsistence cultivation. The northern parts of the Sahel are dominated by open and sparse grass- and shrublands,
88 while cropland, open woody vegetation and deciduous shrublands characterize the southern parts (Breman and
89 Kessler, 1995).

90

91 2.2 CHIRPS rainfall data

92 The CHIRPS v2.0 data set uses TIR (Thermal InfraRed) imager and gauge data, as well as monthly
93 precipitation climatology, CHPClim, and atmospherically modelled rainfall fields from the NOAA Climate
94 Forecast System, version 2 (CFSv2) and TRMM 3B42 (Funk et al., 2015). The CHIRPS data are provided as
95 grids at 0.05° and 0.25° spatial resolutions and extends from 1981 to present. In our study, the CHIRPS data at
96 daily resolution with a spatial resolution of 0.05° were used to extract seasonal rainfall metrics.

97

98 2.3 Deriving seasonal rainfall metrics

99 The method used to identify the onset and cessation of the wet season is referred to Liebmann et al. (2012)
100 and applicable to multiple datasets for precipitation seasonality analysis across the African continent (Dunning
101 et al., 2016). As was described in Liebmann et al. (2012), the climatology wet season was initially determined
102 by the climatological cumulative daily rainfall anomaly, $A(d)$, calculated from the long-term (2001-2015)
103 average rainfall (R_i) for each day of the calendar year minus the long-term annual-mean daily average (\bar{R}). The
104 day with minimum value (d_s) was defined as the start of the wet season and the maximum point (d_c) marks the
105 end of the wet season.

106 (1)

$$107 \quad (d) = \sum_{i=1}^d R_i - \bar{R}$$

108 Subsequently, the onset and cessation were calculated individually for each year and each grid point. For
109 each year the extraction of the rainfall metrics of the wet season was based on equation (2). The daily
110 cumulative rainfall anomaly $A(D)$ on a certain day (P_i) was computed for each day in the range $d_s - 50$ to $d_c + 50$
111 for each year and the day with minimum value was considered as the onset of the wet season.

112 (2)

$$(D) = \sum_{j=d_s-50}^D P_i - \bar{R}$$

114 Once the onset and cessation dates of the wet season for each year were found, the remaining metrics were
115 calculated (Table 1). Fig. 2a illustrated an example of daily rainfall for the grid point (13.5° N, 5.0° W) in 2001
116 and the corresponding cumulative daily anomaly curves were shown in Fig 2b. The blue and red lines signify
117 $A(d)$ and $A(D)$, respectively. The range of minimum and maximum points in the blue line denoted the
118 climatological wet season (Liebmann et al., 2012). The wet season of each individual year was then determined
119 based on the daily precipitation observations covered by the climatological wet season. Areas where the annual
120 minimum occurs after the 1st of October (desert areas) were excluded from further analysis (Diaconescu et al.,
121 2015).

123 2.4 Estimation of growing season ANPP

124 The MODIS/Terra surface reflectance product (MOD09Q1, collection 6) was used to derive a time series of
125 NDVI for the period 2001-2015. NDVI was calculated from the MODIS red and near-infra red bands (8 day
126 composites). The growing season integrated NDVI (\sum NDVI) was used as a proxy for the growing season ANPP.
127 The method was well established and proven to be a reliable proxy for the growing season ANPP in Sahel
128 (Fensholt et al., 2013; Olsson et al., 2005). The \sum NDVI (defined by the area under the curve delimited by start
129 and end of the season) was derived using the TIMESAT software (Jönsson and Eklundh, 2004), which was a
130 widely used tool to extract vegetation seasonal metrics. For this study, we applied the Savitzky-Golay filter
131 implemented in TIMESAT with the following settings: A window size of 4 was applied and a seasonal parameter
132 of 0.5 to fit one season per year. Both the number of iterations for upper envelope adaptation and strength of the
133 envelope adaptation were set to 2 and the start and end of season were determined as 20% and 50% of the

134 amplitude respectively. The \sum NDVI data was then aggregated to the spatial resolution of CHIRPS (0.05°) using a
135 bilinear resampling method. Both Globeland30 (Chen et al., 2014) and ESA CCI (2010) land cover maps
136 (<https://www.esa-landcover-cci.org/>) were used to mask water bodies, irrigated and flooded areas if one or both
137 of the land cover products indicated the presence of water in a pixel.

138

139 **2.5 Statistical analyses**

140 An exponential regression was used to quantify the relationship between growing season ANPP and
141 seasonal rainfall metrics for the entire study area (Fig. 5) and the non-parametric Spearman's rank correlation
142 coefficient was used to measure the relationship between growing season ANPP and seasonal rainfall metrics as a
143 function of seasonal rainfall amount (Fig. 6). Additionally, Generalized Additive Models (GAMs) implemented
144 using the MGCV package (Wood, 2017) in the *R* computing environment (*R* Team, 2014) were applied to derive
145 smooth response curves with seasonal rainfall amount as the explanatory variable and the linear coefficients
146 (averaged over 10 mm rainfall steps) as the response variable (Fig. 7). The models were parameterized assuming
147 normal error distributions. Furthermore, a random forest ensemble learning method (Breiman, 2001) was used to
148 analyze the relative importance of individual seasonal rainfall metrics on growing season ANPP as a function of
149 the seasonal rainfall amount (Fig. 8a). This algorithm produces multiple decision trees based on bootstrapped
150 samples and the nodes of each tree are built up by an iterative process of choosing and splitting nodes to achieve
151 maximum variance reduction. Thus the metrics with highest difference are considered as the most important
152 factors. All pixels based on 15-year averages of seasonal rainfall metrics and ANPP were used for this analysis.
153 Additionally, a multiple regression analysis was applied to identify and map the spatial distribution of the relative
154 importance of the three most important seasonal rainfall metrics (onset and cessation of the wet season and rainy
155 days) explaining the growing season ANPP at the per-pixel level (based on a 15-year time series) (Fig. 8b).

156 A piecewise regression was used to identify breakpoints (Muggeo, 2003), i.e. critical thresholds in the
157 relationship between rainfall metrics and vegetation growth (Fig. 9). A breakpoint is an indication that the
158 vegetation response to changes in a given rainfall metric surpasses a threshold beyond which vegetation
159 functioning is significantly altered. Such a threshold, at the level of individual rainfall seasonality metric,
160 provides an indication of rainfall conditions beyond which vegetation does not tolerate further stress without a
161 marked impact on the growing season ANPP. The 95th percentile of \sum NDVI was selected to represent the
162 potential vegetation productivity attainable for a given seasonal rainfall metric (Donohue et al., 2013). Seasonal
163 rainfall metrics were binned according to the dynamic range of the individual metrics and the average 95th
164 percentile of \sum NDVI was calculated for each bin (for onset, cessation and RD bins with an interval of 1 were
165 used; for SDII a bin of 0.3 was applied; for R95sum bin intervals were set to 0.02; finally we used bins 0.5 for
166 CDD). The breakpoint regression was then applied to the potential vegetation productivity and corresponding
167 seasonal rainfall metrics.

168

169 **2.6 Data availability**

170 The CHIRPS data are available at <http://chg.geog.ucsb.edu/data/chirps/>. The MODIS surface Reflectance
171 product (MOD09Q1) can be downloaded at [https://lpdaac.usgs.gov/dataset_discovery/modis/
172 modis_products_table](https://lpdaac.usgs.gov/dataset_discovery/modis/modis_products_table). The global land cover 30 is available at <http://www.globeland30.org/> and ESA CCI land
173 cover is accessed from <https://www.esa-landcover-cci.org/>.

174

175

176 **3 Results**

177 **3.1 Spatial pattern of seasonal rainfall metrics**

178 A clear north-south gradient was observed for the onset, rainy days (RD), heavy rainfall events (R95sum) and
179 consecutive dry days (CDD) based on a 15-year (2001-2015) average value, with an earlier onset, more rainy
180 days and less heavy rainfall events towards the south (Fig.3a,c,e). The cessation of the wet season (Fig.3b)
181 showed some longitudinal differences with the latest dates found in the eastern Sahel, followed by the western
182 Sahel and the central Sahel showing the earliest cessation dates. A considerable difference between southeastern
183 and southwestern Sahel (Fig. 3d) was observed in the rainfall intensity (SDII). The relatively low rainfall
184 intensity in the southeastern Sahel was mirrored by considerably higher numbers of rainy days.

185

186 **3.2 General response of growing season ANPP to rainfall metrics**

187 The median growing season ANPP clearly followed the mean seasonal rainfall gradient (Fig.4) with other
188 biotic and abiotic factors (e.g. soil texture, nutrients, species composition, fire regime and seasonal rainfall
189 distribution) causing a wide range of values as indicated by the different quantile values.

190

191 The relationships between all the rainfall metrics and growing season ANPP were found to be significant
192 ($p < 0.001$) and the coefficient of determination (r^2) modelled by exponential regression varied between 0.27 and
193 0.73 (Fig.5). For the region as a whole, the number of rainy days was identified as the most important metric
194 impacting on the growing season ANPP ($r^2 = 0.73$) (Fig.5c), closely followed by heavy rainfall events (R95sum)
195 ($r^2 = 0.72$) (Fig.5e), consecutive dry days (CDD) ($r^2 = 0.54$) (Fig.5f) and cessation ($r^2 = 0.37$) (Fig.5b) of the wet
196 season. The impact of the onset on growing season ANPP was also relatively strong ($r^2 = 0.47$) (Fig.5a), whereas
197 a rather weak relationship was observed between growing season ANPP and rainfall intensity (SDII) ($r^2 = 0.27$)
198 (Fig.5d). For all seasonal rainfall metrics except RD, R95sum and CCD, the plots showed some signs of a

199 bimodal distribution of the points, which was caused by the differences in the east-west patterns of the spatial
200 distribution of seasonal rainfall metrics (onset, cessation and SDII) in Sahel as reported in Fig.3.

201

202 **3.3 Response of growing season ANPP to seasonal rainfall metrics along the rainfall gradient**

203 Although the relationship between growing season ANPP and seasonal rainfall amount (R) obviously changed
204 along the rainfall gradient (Fig. 4), variations in seasonal rainfall distribution (e.g., onset and R95sum) can cause
205 considerable changes in growing season ANPP under the same rainfall gradient (Fig. 5). The influence of
206 seasonal rainfall distribution on growing season ANPP was thus analyzed under different mean annual rainfall
207 values along the north (low rainfall) to south (high rainfall) gradient (Fig. 6). The dependency of growing season
208 ANPP on seasonal rainfall metrics was clearly seen to be a function of the seasonal rainfall amount. Below ~300
209 mm yr⁻¹, the vegetation seems to be stable and rather insensitive to variations of the rainfall metrics, however,
210 above 300 mm yr⁻¹, the impacts can be clearly seen by a larger spread in growing season ANPP values for a given
211 amount of seasonal rainfall (Fig. 6). For example, the growing season ANPP decreased strongly with a later onset,
212 an earlier cessation of the wet season, a smaller number of rainy days, a higher rainfall intensity, more heavy
213 rainfall events and longer dry spells. Above ~700 mm yr⁻¹, the vegetation showed again a reduced sensitivity to
214 variations of the wet season by a convergence of growing season ANPP values irrespective of the seasonal
215 rainfall metric value.

216

217 The non-parametric Spearman's rank correlation coefficient was used to quantify the strength of the impact
218 of individual seasonal rainfall metrics on growing season ANPP as a function of seasonal rainfall (Fig. 7). In
219 general, the impacts of rainfall metrics on vegetation were distinctive along the 100-800 mm yr⁻¹ gradient with a
220 peak in r values (respectively positive or negative dependent on the rainfall metric) for most metrics around 650
221 mm yr⁻¹ followed by a sharp drop-off (Fig. 7). It should be noted that modelling uncertainties increased for all

222 rainfall metrics due to fewer observations in the lowermost seasonal rainfall total bins. For the wet season the
223 pattern of RD, SDII, R95sum and CDD showed a sharp decrease in r values from 100-300 mm yr⁻¹. The number
224 of consecutive dry days (CDD) showed moderate r values balancing around zero generally indicating less
225 importance of the CDD variable on growing season ANPP along the rainfall gradient analyzed.

226

227

228 The relative importance of the individual rainfall metrics on growing season ANPP was assessed based on a
229 random forest model (Fig. 8a). The explained variance of growing season ANPP explained by rainfall metrics
230 (blue line in Fig. 8a) was increasing with mean annual rainfall up to 600-700 mm yr⁻¹ from where the degree of
231 explained variance decreases, which corresponds with the results presented in Fig. 4 (the widest belt of the
232 quantile values was observed for rainfall of 600-700 mm yr⁻¹, suggesting that the seasonal rainfall metrics
233 additional to the seasonal rainfall amount was increasingly important in this rainfall zone) and in Fig. 7. The
234 cessation of the wet season was identified as the most important factor controlling growing season ANPP in
235 semi-arid areas of Sahel (400-700 mm yr⁻¹), followed by the onset and number of rainy days. As measured by the
236 relative importance, these three rainfall metrics together accounted for 60-70% of the variance explained by all
237 rainfall metrics for all seasonal rainfall amounts. In arid areas (100-300 mm yr⁻¹) the number of rainy days was
238 found to be the most important variable.

239

240 The spatial distribution of the relative importance of the onset and cessation of the wet season and number of
241 rainy days on growing season ANPP was identified at the pixel-level for 2001 to 2015 (Fig. 8b). At Sahel scale,
242 the number of rainy days (bluish colors) was observed to be the dominating factor, followed by the onset of the
243 wet season (reddish colors) and cessation (greenish colors). There were no clear signs of a latitudinal or
244 longitudinal dependency on which rainfall metric was dominating, but some clustering was evident with a

245 predominance of rainy days influence in the Western Sahel with limited influence by the cessation date on the
246 growing season ANPP.

247

248 **3.4 Critical points for growing season ANPP**

249 A piecewise regression between growing season ANPP and seasonal rainfall metrics was applied to identify
250 if critical breakpoints in the relationship between growing season ANPP and rainfall metrics exist (Fig. 9). We
251 found that the most evident thresholds (average values for the Sahel zone) in relation to seasonal rainfall metrics
252 influence on growing season ANPP relate to the onset of the wet season (Fig. 9a), the rainfall intensity (SDII)
253 (Fig. 9d) and consecutive dry days (CDD) (Fig. 9f). If the onset of the wet season was later than day of year 140
254 this will have an increasingly negative effect on growing season ANPP as a function of the onset delay and
255 contrastingly if the onset starts earlier than day of year 140 this will also have an increasingly adverse effect on
256 growing season ANPP. Also, an optimum of rainfall intensity of 13 mm day⁻¹ was detected; if rainfall intensity
257 exceeds 13 mm day⁻¹, vegetation productivity starts to be negatively affected, whereas a lower intensity will also
258 negatively impact on growing season ANPP. There was a pronounced decline in growing season ANPP as a
259 function of number of consecutive dry days. However, when CDD exceeds ~14 days a breakpoint in the curve
260 was detected, as dry spells of this magnitude led to a strong reduction in vegetation growth. The number of rainy
261 days (Fig. 9c) was linearly related to growing season ANPP until 69 days, beyond which RD became less
262 decisive for the amount of growing season ANPP. Similarly, heavy rainfall events (fraction of annual rainfall
263 events exceeding the 95th percentile) (Fig. 9e) were negatively related to growing season ANPP, until a certain
264 threshold (larger than 0.80), from where the vegetation loses sensitivity to the impact from an increased
265 frequency of heavy rainfall events. Finally, the cessation date of the wet season (Fig. 9b) was shown to be nearly
266 linearly related to growing season ANPP. A breakpoint was detected by the piecewise regression algorithm

267 around day 285, beyond which the delay in cessation date was slightly more favorable for higher growing season
268 ANPP yields as compared to a cessation date before day 285.

269

270 **4 Discussion**

271 This study presents first empirical evidence on the impact of rainfall seasonality on vegetation productivity at
272 regional scale and the results provide a clear picture on the importance of six seasonal rainfall metrics on growing
273 season ANPP under different rainfall conditions (i.e. mean annual rainfall). Uncertainty in the rainfall data is
274 inevitably to have an impact on the extraction of seasonal rainfall metrics which further impacts the relationship
275 between seasonal rainfall metrics and ANPP. Based on improved climatologies systematic bias in the CHIRPS
276 dataset has been removed and the data is considered state-of-the-art within quasi-global, high spatial resolution
277 rainfall datasets (Funk et al., 2015). As this study does not address temporal changes in the seasonal rainfall
278 metrics or \sum NDVI, but merely presents results on the general coupling between rainfall metrics and vegetation
279 productivity, we consider the results to be statistically robust. We conducted a parallel set of analyses based on
280 the RFE-2.0 rainfall product developed by the NOAA Climate Prediction Center (CPC) (Herman et al., 1997),
281 which, like CHIRPS, is also a gauge-satellite blended and the outcome of these analyses (not shown) yielded
282 nearly similar results as to what was presented here. At the same time \sum NDVI derived from MODIS will also be
283 impacted from cloud cover during the growing season, but the use of the Savitzky-Golay filtering algorithm has
284 proven to be an effective way of overcoming residual noise effects in the NDVI time-series (Fensholt et al., 2015).

285 The Sahel zone is often defined from isohyets of annual rainfall as a common denominator of the hydrological
286 conditions of the region. It was however shown here, that considerable east-west differences occurred in several
287 of the seasonal rainfall metrics analyzed with a much higher number of rainy days and corresponding lower
288 rainfall intensity in the southeastern Sahel as compared to the southwestern part. Variability in the rainfall
289 intensity was shown here to influence the growing season ANPP generated over a growing season (Fig. 9d) and

290 hence spatio-temporal changes in rainfall intensity (but characterized by the same amount of seasonal rainfall)
291 will impact vegetation productivity. This has important implications for the use of the rain use efficiency (RUE)
292 (Houerou, 1984) or Residual Trend Analysis (RESTREND) approach (regressing $\sum\text{NDVI}$ from annual
293 precipitation and subsequently calculating the residuals as the difference between observed $\sum\text{NDVI}$ and $\sum\text{NDVI}$
294 as predicted from annual precipitation) (Evans and Geerken, 2004), which is derived from annually or seasonally
295 summed rainfall and commonly used as an indicator for land degradation (Archer, 2004; Bai et al., 2008;
296 Fensholt and Kjeld, 2011; Prince et al., 1998; Ratzmann et al., 2016; Wessels et al., 2007) as discussed in
297 Ratzmann et al. (2016). Interestingly, a limited impact of rainfall seasonality on growing season ANPP was found
298 in arid lands below 300 mm yr⁻¹ rainfall, suggesting that the species composition was adapted to rainfall variation,
299 and that the rather sparse vegetation cover was able to effectively utilize rainfall independent of the seasonal
300 distribution. This was very different in the semi-arid and northern sub-humid zone (300-700 mm yr⁻¹), where
301 variations in rainfall seasonality were found to be more closely linked with variations in growing season ANPP.
302 This implied that a favorable distribution of rainfall may lead to increased productivity, as it was observed in
303 Senegal between 2006 and 2011 (Brandt et al., 2017), but below average rainfall conditions with an unfavorable
304 distribution led to an immediate reduction in vegetation cover and growing season ANPP.

305 Not surprisingly, the number of rainy days showed the highest relationship with growing season ANPP (Fig.
306 5c), with increasing productivity along with increasing rainy days, up to 69 days, where the relation weakens (Fig.
307 9c). The importance of this metric was closely followed by the heavy rainfall events, which were negatively
308 correlated with growing season ANPP (Fig. 5e), and decreases the productivity until heavy rainfall events
309 reached a share of 80%, which led to a constant level of low vegetation productivity (Fig. 9e). The importance of
310 the timing of the wet season, i.e. the onset and cessation, increases rapidly along the rainfall gradient, having the
311 highest impact on growing season ANPP in the semi-arid zone (300-700 mm yr⁻¹). The reason for the importance
312 of the timing of the onset of the growing season on the growing season ANPP (Fig. 9a) with an almost linear

313 decrease in growing season ANPP as a function of onset delay should be found in the predominance of annual
314 grasses which are photoperiodic (Penning de Vries and Djiteye, 1982). The cessation of season was thus
315 controlled by day length and do therefore not compensate for a delay in the onset. Also, a too early onset was
316 found to decrease growing season ANPP, which is likely to be associated with so-called “false starts” of the
317 growing season. Often, an early start of the growing season is accompanied by a significant number of dry-days
318 occurring shortly after the start of the wet season with a detrimental impact upon plant growth (Proud and
319 Rasmussen, 2011). Finally, we found that the general impact of consecutive dry days was difficult to quantify
320 (Fig.7f). However, a rather clear critical threshold of 14 consecutive days without rainfall was found to have an
321 increased adverse impact on the growing season ANPP. This threshold of 14 days as an average for Sahel was
322 related to the depletion time of the upper layer soil water and the root depth of the herbaceous stratum (primarily
323 annual grasses) but will vary spatially with different soil and vegetation types (Penning de Vries and Djiteye,
324 1982).

325 Several studies have reported a tendency towards an earlier start of the wet season (Sanogo et al., 2015; Zhang
326 et al., 2017), but projections predict a delay of the wet season in the later 21th century (Biasutti and Sobel, 2009;
327 Guan et al., 2014). Moreover, an increase in heavy rainfall events and prolonged dry spells were observed and
328 projected for the future (Sanogo et al., 2015; Taylor et al., 2017; Zhang et al., 2017). Our results showed that the
329 semi-arid zone will be most prone to these projected changes, and an increase in heavy rainfall events, a delay in
330 the onset of the wet season and dry spells exceeding 14 days will cause a significant reduction in vegetation
331 productivity, although the annual rainfall amount may be constant or even increasing. Disregarding the
332 importance and impact of varying rainfall distribution on vegetation productivity leads to a bias in any ANPP
333 prediction, and this knowledge should be implemented in any prediction and estimation of ANPP, both for
334 ecosystem models and remote sensing based analyses, especially in the context of food security. Although this
335 study did not include a temporal change component of the metrics analyzed, the length of high quality time series

336 data of both vegetation productivity and rainfall with a daily temporal resolution does provide the possibility for
337 adding a temporal dimension which will be pursued in a future study.

338

339 **5 Summary and conclusion**

340 In this study we analyzed the impact of seasonal rainfall distribution (represented by onset and cessation of the
341 wet season, number of rainy days, rainfall intensity, number of consecutive dry days and heavy rainfall events) on
342 growing season ANPP for the Sahelian zone. Overall, a clear north-south gradient was observed for the onset,
343 rainy days, heavy rainfall events and consecutive dry days, but also considerable differences in cessation date,
344 number of rainy days and the rainfall intensity were observed between Eastern and Western Sahel. We found the
345 strongest relationship between growing season ANPP and the number of rainy days ($r^2=0.73$), closely followed
346 by a relationship between growing season ANPP and heavy rainfall events ($r^2=0.72$). Growing season ANPP in
347 the arid zone (100-300 mm yr⁻¹) was rather insensitive to variations in the seasonal rainfall metrics, whereas
348 vegetation in the semi-arid zone (300-700 mm yr⁻¹) was significantly impacted by most metrics, especially by the
349 number of rainy days and timing (onset and cessation) of the wet season. Finally, the critical breakpoints analysis
350 between growing season ANPP and all rainfall metrics showed that the growing season ANPP were particularly
351 negatively impacted after >14 consecutive dry days and that a rainfall intensity of 13 mm day⁻¹ was detected for
352 optimum growing season ANPP. Overall, it can be concluded that seasonal rainfall distribution significantly
353 influence ANPP and the effect of different rainfall metrics was observed to vary along the north-south rainfall
354 gradient. These findings have important implications for the sheer amount of dryland studies in which annually or
355 seasonally summed rainfall and ANPP are used to derive indicators of land degradation or anthropogenic
356 influence (e.g. the use of RUE and RESTREND). When studying subtle changes in dryland vegetation
357 productivity based on time series of satellite data, as caused by both climate and anthropogenic forcing, it is
358 essential also to consider the potential effect from changes in the rainfall regime as expressed in the seasonal

359 rainfall metrics studied here. Inter-annual differences in the seasonal distribution of rainfall is known to have an
360 impact on species composition in Sahel (Mbow et al., 2013) and it is likely that the herbaceous vegetation is able
361 to adapt to changes seasonal rainfall distribution expressed by a shift in the abundance of species favored by
362 increased heavy rainfall events and longer dry spells.

363

364 *Competing interests.* The authors declare that they have no conflict of interest.

365

366 *Acknowledgements.* This study is jointly supported by the European Union’s Horizon 2020 research and
367 innovation programme under the Marie Skłodowska-Curie grant agreement (project BICSA number 656564),
368 China Scholarship Council (CSC, 201506190076), and the Danish Council for Independent Research (DFR)
369 project: Greening of drylands: Towards understanding ecosystem functioning changes, drivers and impacts on
370 livelihoods, and Chinese National Science and Technology Major Project (03-Y20A04-9001-15/16). Also, we
371 would like to thank the associate editor Jochen Schöngart, the reviewer M.Marshall and the anonymous reviewer
372 for providing detailed comments and constructive suggestions.

373

374 **Reference**

375 Abdi, A. M., Seaquist, J., Tenenbaum, D. E., Eklundh, L. and Ardö, J.: The supply and demand of net primary
376 production in the Sahel, *Environmental Research Letters*, 9(9), 94003, doi:10.1088/1748-9326/9/9/094003, 2014.

377 Archer, E.: Beyond the “climate versus grazing” impasse: using remote sensing to investigate the effects of
378 grazing system choice on vegetation cover in the eastern, *Journal of Arid Environments*, 57(3), 381–408,
379 doi:10.1016/S0140-1963(03)00107-1, 2004.

380 Bai, Z., Dent, D. and Olsson, L.: Proxy global assessment of land degradation, *Soil use and Management*, 24,
381 223–234, doi:10.1111/j.1475-2743.2008.00169.x, 2008.

382 Bates, J. D., Svejcar, T., Miller, R. F. and Angell, R. A.: The effects of precipitation timing on sagebrush
383 steppe vegetation, *Journal of Arid Environments*, 64(4), 670–697, doi:10.1016/j.jaridenv.2005.06.026, 2006.

384 Biasutti, M. and Sobel, A. H.: Delayed Sahel rainfall and global seasonal cycle in a warmer climate,
385 *Geophysical Research Letters*, 36(23), 1–5, doi:10.1029/2009GL041303, 2009.

386 Brandt, M., Tappan, G., Diouf, A., Beye, G. and Mbow, C.: Woody vegetation die off and regeneration in
387 response to rainfall variability in the West African Sahel, *Remote Sensing*, 9, 39, doi:10.3390/rs9010039, 2017.

388 Breiman, L.: Random forests, *Machine Learning*, 45(1), 5–32, doi:10.1023/A:1010933404324, 2001.

389 Breman, H. and Kessler, J.: *Woody Plants in Agro-Ecosystems of Semi-Arid Regions: with an Emphasis on*
390 *the Sahelian Countries*, Springer Berlin Heidelberg, 1995.

391 Chen, J., Chen, J., Liao, A., Cao, X., Chen, L., Chen, X., He, C., Han, G., Peng, S., Lu, M., Zhang, W., Tong,
392 X. and Mills, J.: Global land cover mapping at 30 m resolution: A POK-based operational approach, *ISPRS*
393 *Journal of Photogrammetry and Remote Sensing*, 103, 7–27, doi:10.1016/j.isprsjprs.2014.09.002, 2014.

394 Diaconescu, E. P., Gachon, P., Scinocca, J. and Laprise, R.: Evaluation of daily precipitation statistics and
395 monsoon onset/retreat over western Sahel in multiple data sets, *Climate Dynamics*, 45(5–6), 1325–1354,
396 doi:10.1007/s00382-014-2383-2, 2015.

397 Diouf, A. A., Hiernaux, P., Brandt, M., Faye, G., Djaby, B., Diop, M. B., Ndione, J. A. and Tychon, B.: Do
398 agrometeorological data improve optical satellite-based estimations of the herbaceous yield in Sahelian semi-arid
399 ecosystems?, *Remote Sensing*, 8(8), 668, doi:10.3390/rs8080668, 2016.

400 Donohue, R. J., Roderick, M. L., McVicar, T. R. and Farquhar, G. D.: Impact of CO₂ fertilization on
401 maximum foliage cover across the globe’s warm, arid environments, *Geophysical Research Letters*, 40(12),
402 3031–3035, doi:10.1002/grl.50563, 2013.

403 Dunning, C. M., Black, E. C. L. and Allan, R. P.: The onset and cessation of seasonal rainfall over Africa,
404 *Journal of Geophysical Research: Atmospheres*, 121, 11,405–11,424, doi:10.1002/2016JD025428, 2016.

405 Evans, J. and Geerken, R.: Discrimination between climate and human-induced dryland degradation, *Journal*
406 *of Arid Environments*, 57(4), 535–554, doi:10.1016/S0140-1963(03)00121-6, 2004.

407 Fay, P. A., Carlisle, J. D., Knapp, A. K., Blair, J. M. and Collins, S. L.: Altering rainfall timing and quantity in
408 a mesic grassland ecosystem: Design and performance of rainfall manipulation shelters, *Ecosystems*, 3(3), 308–
409 319, doi:10.1007/s100210000028, 2000.

410 Fensholt, R. and Kjeld, R.: Analysis of trends in the Sahelian “rain-use efficiency” using GIMMS NDVI, RFE
411 and GPCP rainfall data, *Remote Sensing of Environment*, 115(2), 438–451, doi:10.1016/j.rse.2010.09.014, 2011.

412 Fensholt, R., Rasmussen, K., Kaspersen, P., Huber, S., Horion, S. and Swinnen, E.: Assessing land
413 degradation/recovery in the African Sahel from long-term earth observation based primary productivity and
414 precipitation relationships, *Remote Sensing*, 5(2), 664–686, doi:10.3390/rs5020664, 2013.

415 Fensholt, R., Horion, S., Tagesson, T., Ehammer, A., Grogan, K., Tian, F., Huber, S., Verbesselt, J., Prince, S.
416 P., Tucker, C. J. and Rasmussen, K.: Assessment of Vegetation Trends in Drylands from Time Series of Earth
417 Observation Data, *Remote Sensing Time Series*, 2015.

418 Field, C.: Managing the risks of extreme events and disasters to advance climate change adaptation, IPCC
419 special report of the intergovernmental panel on climate change, 2012.

420 Fischer, E. M., Beyerle, U. and Knutti, R.: Robust spatially aggregated projections of climate extremes,
421 *Nature Climate Change*, 3(12), 1033–1038, doi:10.1038/nclimate2051, 2013.

422 Fitzpatrick, R. G. J., Bain, C. L., Knippertz, P., Marsham, J. H. and Parker, D. J.: The West African monsoon
423 onset: A concise comparison of definitions, *Journal of Climate*, 28(22), 8673–8694, doi:10.1175/JCLI-D-15-
424 0265.1, 2015.

425 Funk, C., Peterson, P., Landsfeld, M., Pedreros, D., Verdin, J., Shukla, S., Husak, G., Rowland, J., Harrison,
426 L., Hoell, A. and Michaelsen, J.: The climate hazards infrared precipitation with stations—a new environmental
427 record for monitoring extremes, *Scientific Data*, 2, 150066, doi:10.1038/sdata.2015.66, 2015.

428 Guan, K., Good, S. P., Caylor, K. K., Sato, H., Wood, E. F. and Li, H.: Continental-scale impacts of intra-
429 seasonal rainfall variability on simulated ecosystem responses in Africa, *Biogeosciences*, 11(23), 6939–6954,
430 doi:10.5194/bg-11-6939-2014, 2014.

431 Herman, A., Kumar, V. B., Arkin, P. A. and Kousky, J. V.: Objectively determined 10-day African rainfall
432 estimates created for famine early warning systems, *International Journal of Remote Sensing*, 18(February),
433 2147–2159, doi:10.1080/014311697217800, 1997.

434 Herrmann, S. M., Anyamba, A. and Tucker, C. J.: Recent trends in vegetation dynamics in the African Sahel
435 and their relationship to climate, *Global Environmental Change*, 15(4), 394–404,
436 doi:10.1016/j.gloenvcha.2005.08.004, 2005.

437 Houerou, H. Le: Rain use efficiency: a unifying concept in arid-land ecology, *Journal of Arid Environments*,
438 7(3), 213–247, 1984.

439 Huber, S., Fensholt, R. and Rasmussen, K.: Water availability as the driver of vegetation dynamics in the
440 African Sahel from 1982 to 2007, *Global and Planetary Change*, 76(3–4), 186–195,
441 doi:10.1016/j.gloplacha.2011.01.006, 2011.

442 Jönsson, P. and Eklundh, L.: TIMESAT—a program for analyzing time-series of satellite sensor data,
443 *Computers & Geosciences*, 30, 833–845, 2004.

444 Kaspersen, P. S., Fensholt, R. and Huber, S.: A spatiotemporal analysis of climatic drivers for observed
445 changes in Sahelian vegetation productivity (1982–2007), *International Journal of Geophysics*, 2011, 1–14,
446 doi:10.1155/2011/715321, 2011.

447 Kharin, V. V., Zwiers, F. W., Zhang, X. and Hegerl, G. C.: Changes in temperature and precipitation extremes
448 in the IPCC ensemble of global coupled model simulations, *Journal of Climate*, 20(8), 1419–1444,
449 doi:10.1175/JCLI4066.1, 2007.

450 Lebel, T. and Ali, A.: Recent trends in the Central and Western Sahel rainfall regime (1990–2007), *Journal of*

451 Hydrology, 375(1), 52–64, doi:10.1016/j.jhydrol.2008.11.030, 2009.

452 Leisinger, K. M. and Schmitt, K.: Survival in the Sahel: An ecological and developmental challenge,
453 International Service for National Agricultural Research, 1995.

454 Liebmann, B., Bladé, I., Kiladis, G. N., Carvalho, L. M. V, Senay, G. B., Allured, D., Leroux, S. and Funk, C.:
455 Seasonality of African precipitation from 1996 to 2009, *Journal of Climate*, 25(12), 4304–4322,
456 doi:10.1175/JCLI-D-11-00157.1, 2012.

457 Mbow, C., Fensholt, R., Rasmussen, K. and Diop, D.: Can vegetation productivity be derived from greenness
458 in a semi-arid environment? Evidence from ground-based measurements, *Journal of Arid Environments*, 97, 56–
459 65, doi:10.1016/j.jaridenv.2013.05.011, 2013.

460 Muggeo, V. M. R.: Estimating regression models with unknown break-points, *Statistics in Medicine*, 22(19),
461 3055–3071, doi:10.1002/sim.1545, 2003.

462 Nicholson, S. E.: The nature of rainfall variability over Africa on time scales of decades to millenia, *Global
463 and Planetary Change*, 26(1–3), 137–158, doi:https://doi.org/10.1016/S0921-8181(00)00040-0, 2000.

464 Olsson, L., Eklundh, L. and Ardö, J.: A recent greening of the Sahel—trends, patterns and potential causes,
465 *Journal of Arid Environments*, 63(3), 556–566, doi:10.1016/j.jaridenv.2005.03.008, 2005.

466 Panthou, G., Vischel, T. and Lebel, T.: Recent trends in the regime of extreme rainfall in the Central Sahel,
467 *International Journal of Climatology*, 34(15), 3998–4006, doi:10.1002/joc.3984, 2014.

468 Penning de Vries, F. W. T. and Djiteye, M. A.: The productivity of Sahelian rangeland: a study of soils,
469 vegetation and the exploitation of this natural resource, Centre for Agricultural Publishing and Documentation,
470 Wageningen, Netherlands, 1982.

471 Prince, S., Colstoun, D. and Brown, E.: Evidence from rain-use efficiencies does not indicate extensive
472 Sahelian desertification, *Global Change Biology*, 4(4), 359–374, doi:10.1046/j.1365-2486.1998.00158.x, 1998.

473 Proud, S. R. and Rasmussen, L. V.: The influence of seasonal rainfall upon Sahel vegetation, *Remote Sensing*

474 Letters, 2(3), 241–249, doi:10.1080/01431161.2010.515268, 2011.

475 Ratzmann, G., Gangkofner, U., Tietjen, B. and Fensholt, R.: Dryland vegetation functional response to altered
476 rainfall amounts and variability derived from satellite time series data, *Remote Sensing*, 8, 1026,
477 doi:10.3390/rs8121026, 2016.

478 Rishmawi, K., Prince, S. and Xue, Y.: Vegetation Responses to Climate Variability in the Northern Arid to
479 Sub-Humid Zones of Sub-Saharan Africa, *Remote Sensing*, 8(11), 910, doi:10.3390/rs8110910, 2016.

480 R Team.: R: A language and environment for statistical computing. Vienna, Austria: R Foundation for
481 Statistical Computing, <http://www.R-project.org/>, 2014.

482 Romankiewicz, C., Doevenspeck, M., Brandt, M. and Samimi, C.: Adaptation as by-product: Migration and
483 environmental change in Nguith, Senegal, *Journal of the Geographical Society of Berlin*, 147(2), 95–108,
484 doi:10.12854/erde-147-7, 2016.

485 Sanogo, S., Fink, A. H., Omotosho, J. A., Ba, A., Redl, R. and Ermert, V.: Spatio-temporal characteristics of
486 the recent rainfall recovery in West Africa, *International Journal of Climatology*, 35(15), 4589–4605,
487 doi:10.1002/joc.4309, 2015.

488 Smith, M. D.: The ecological role of climate extremes: Current understanding and future prospects, *Journal of*
489 *Ecology*, 99(3), 651–655, doi:10.1111/j.1365-2745.2011.01833.x, 2011.

490 Taylor, C. M., Belušić, D., Guichard, F., Parker, D. J., Vischel, T., Bock, O., Harris, P. P., Janicot, S., Klein,
491 C. and Panthou, G.: Frequency of extreme Sahelian storms tripled since 1982 in satellite observations, *Nature*,
492 544(7651), 475–478, doi:10.1038/nature22069, 2017.

493 Thomey, M. L., Collins, S. L., Vargas, R., Johnson, J. E., Brown, R. F., Natvig, D. O. and Friggens, M. T.:
494 Effect of precipitation variability on net primary production and soil respiration in a Chihuahuan Desert grassland,
495 *Global change biology*, 17(4), 1505–1515, doi:10.1111/j.1365-2486.2010.02363.x Effect, 2011.

496 Wessels, K., Prince, S., Malherbe, J. and Small, J.: Can human-induced land degradation be distinguished

497 from the effects of rainfall variability? A case study in South Africa, *Journal of Arid Environments*, 68(2), 271–
 498 297, doi:10.1016/j.jaridenv.2006.05.015, 2007.

499 Wood, S.: Package mgcv, <https://cran.r-project.org/web/packages/mgcv/index.html>, 2017.

500 Zhang, W., Brandt, M., Guichard, F., Tian, Q. and Fensholt, R.: Using long-term daily satellite based rainfall
 501 data (1983–2015) to analyze spatio-temporal changes in the sahelian rainfall regime, *Journal of Hydrology*, 550,
 502 427–440, doi:10.1016/j.jhydrol.2017.05.033, 2017.

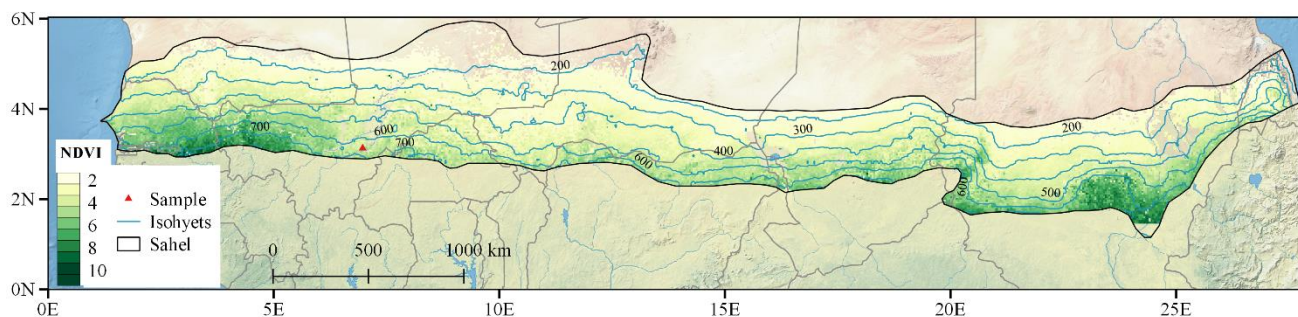
503

504 **Table 1** Rainfall metrics describing the seasonality and extreme events

Index name	Definitions	Units
Onset of wet season (Onset)	The minimum value in the accumulative anomaly of daily rainfall	day of year
Cessation of wet season (Cessation)	The maximum value of the accumulative anomaly of daily rainfall	day of year
Rainy days (RD)	Number of days with rainfall ≥ 1 mm between the onset and the cessation of the wet season	days
Rainfall intensity (SDII)	Ratio of annual total rainfall and number of rainy days ≥ 1 mm	mm day ⁻¹
Heavy rainfall events (R95sum):	Fraction of annual rainfall events exceeding the (2001–2015) 95th percentile	%
Consecutive dry days (CDD):	Maximum number of consecutive days with rainfall < 1 mm during wet season	days
Seasonal rainfall amount (R)	Rainfall amount during the wet season	mm yr ⁻¹

505

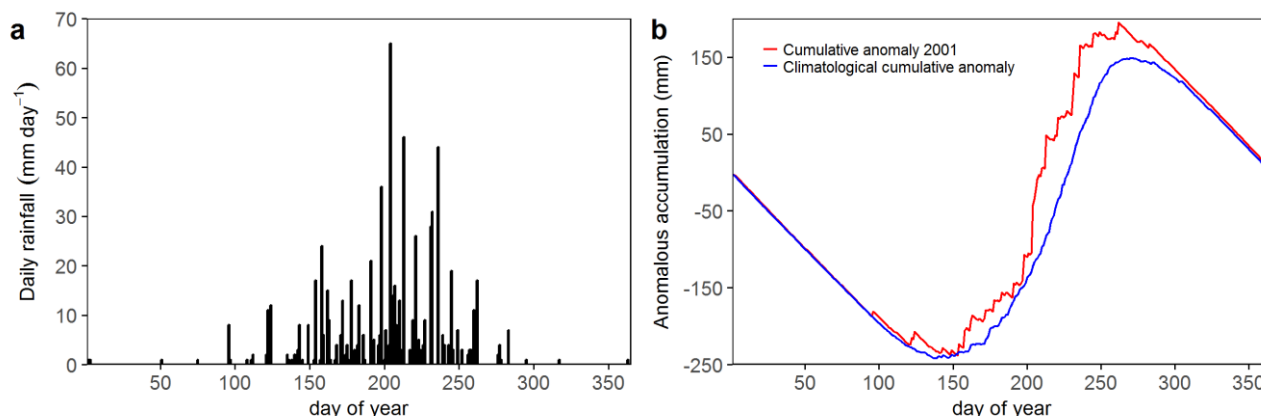
506



507

508 Fig 1. Study area outlining the Sahelian region (black color; 100-800 mm yr⁻¹). Σ NDVI (seasonal integral) is based on a 15-
509 year (2001-2015) average using MODIS data; the red grid point (13.5° N, 5.0° W) is used to illustrate the extractions of onset
510 and cessation of the wet season shown in Fig. 2. Isohyets are based on a 15-year (2001-2015) average of the seasonal rainfall
511 amount (CHIRPS v2.0).

512

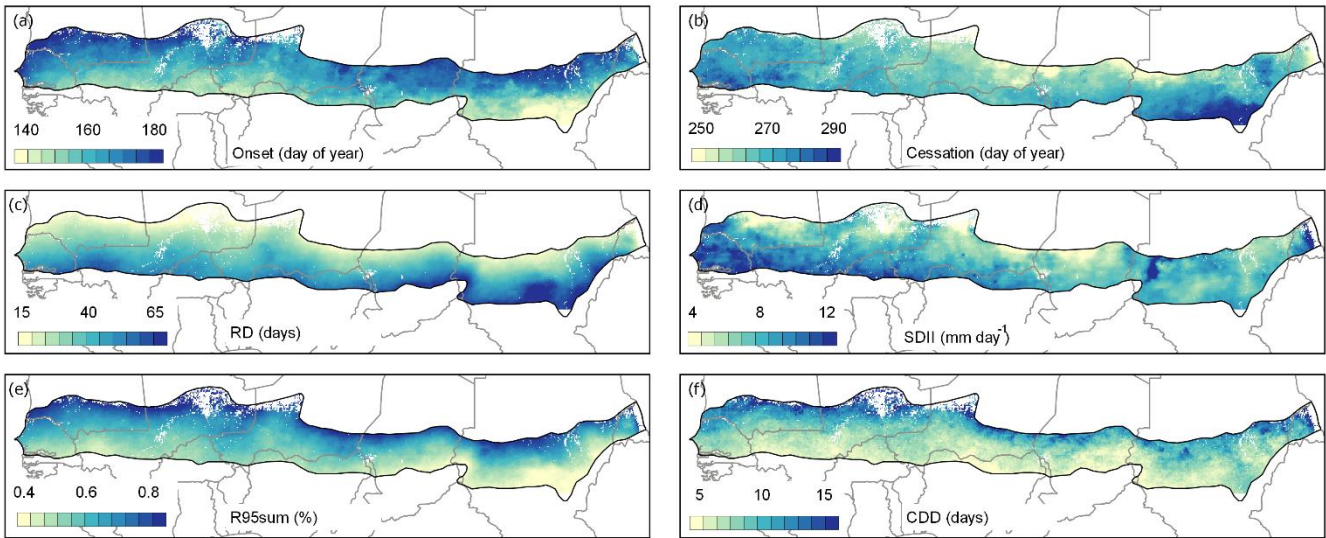


513

514 Fig.2. (a) Daily rainfall distribution and (b) anomalous accumulative curve for the grid point 13.5° N, 5.0° W (shown in Fig.
515 1) for the year of 2001. The blue line (accumulated anomaly) is computed from a 15-year (2001-2015) average of daily
516 rainfall.

517

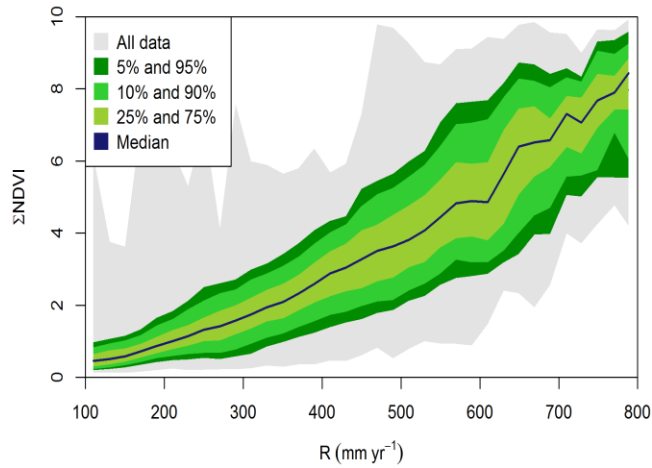
518



519
520

Fig.3. Spatial distribution of average seasonal rainfall metrics a) onset of wet season (day of year); b) cessation of wet season (day of year); c) rainy days (days); d) daily intensity (mm day^{-1}); e) heavy rainfall events (%); f) consecutive dry days (days) based on 15-year averages (2001-2015). Pixels within the study area are masked (white color) in accordance with the description in the methods section.

524

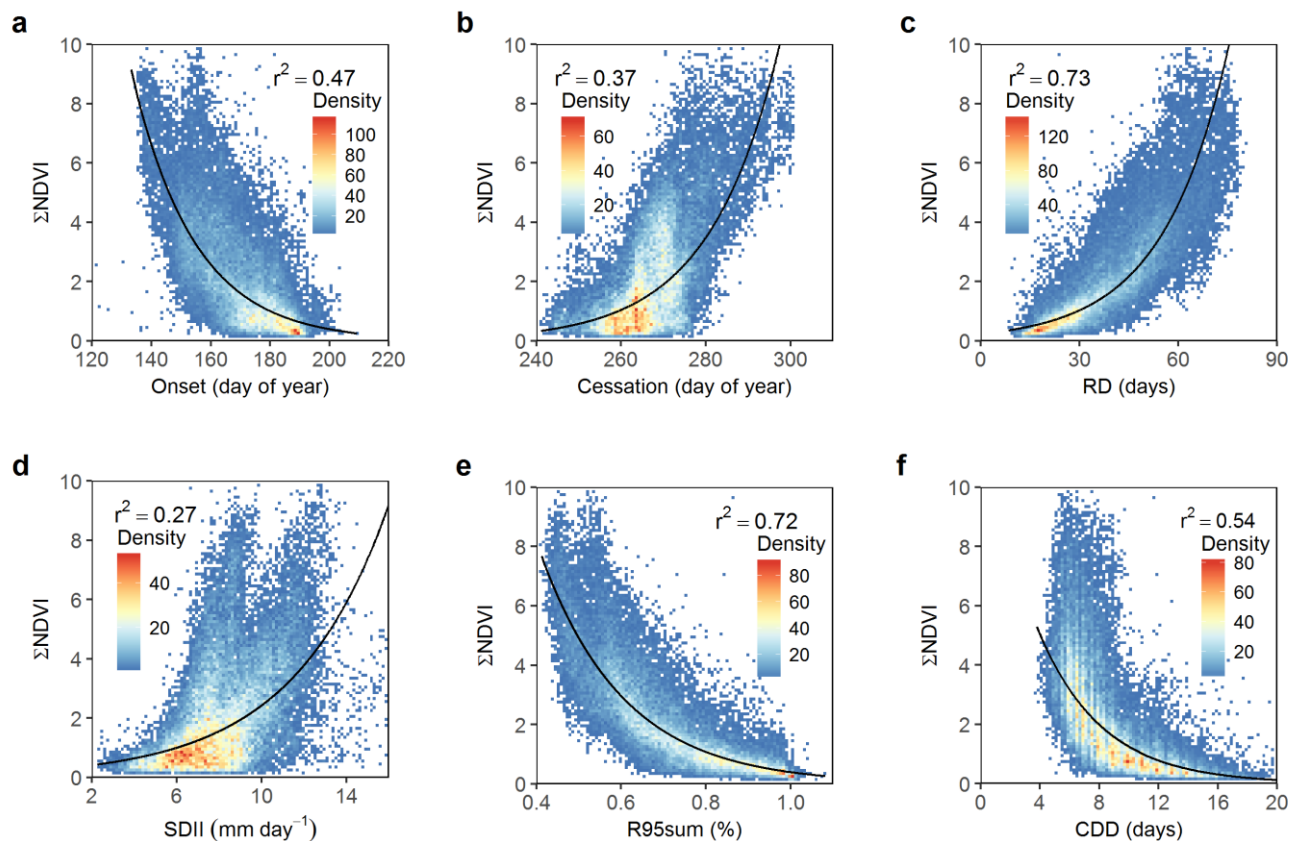


525

526 Fig.4. Growing season ANPP (Σ NDVI) as a function of mean seasonal rainfall amount (R) plotted as quantiles for the Sahel-
527 Sudanian zone (pixel averages for 2001-2015).

528

529

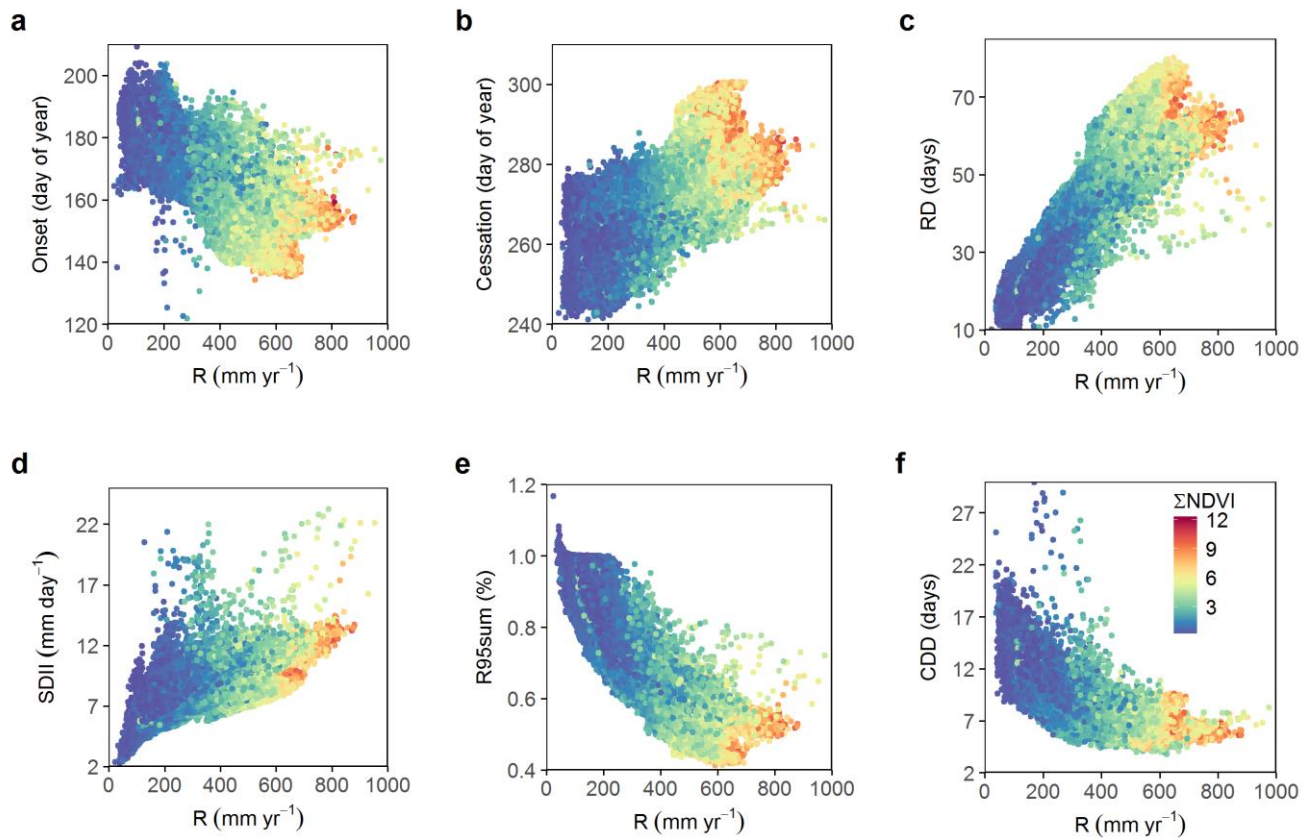


530 Fig.5. Density scatterplot showing the **relationships** between seasonal rainfall metrics and growing season ANPP (Σ NDVI).
531 All analyses are based on 15-year averages (2001-2015). The black lines are exponential regression curves. All points
532 (n=30862) are located between 100 and 800 mm annual rainfall.

534

535

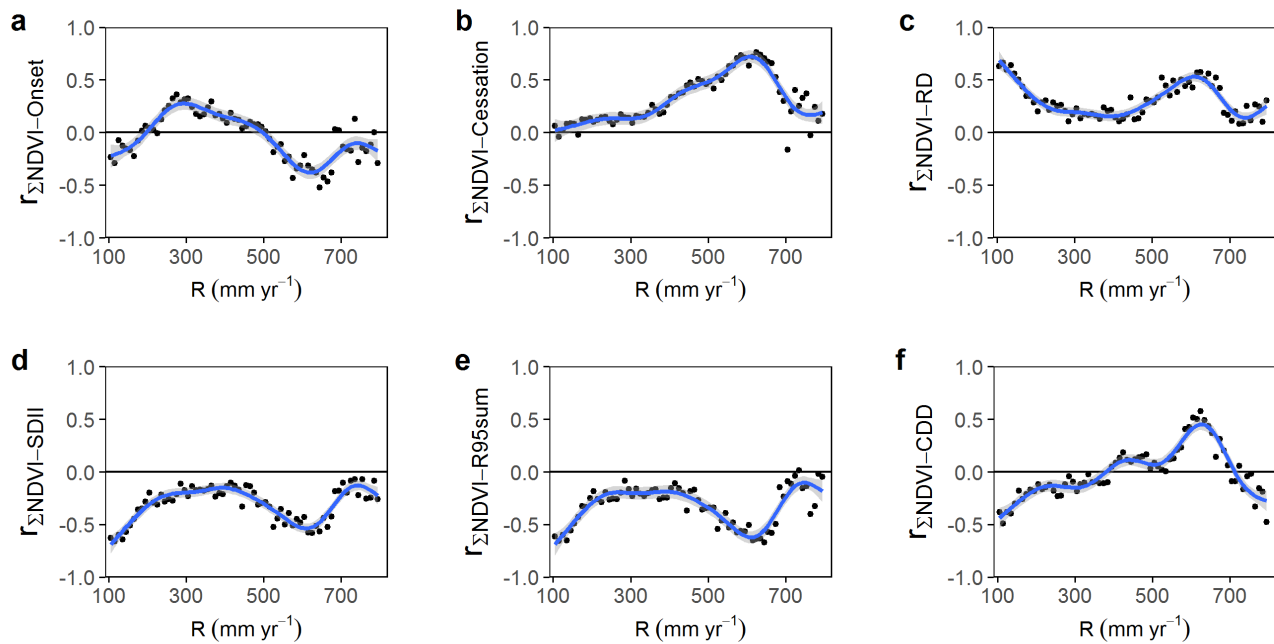
536



537

538 Fig. 6. Relationships between seasonal rainfall metrics and growing season ANPP as a function of seasonal rainfall amount
 539 based on 15-year averages (2001-2015).

540

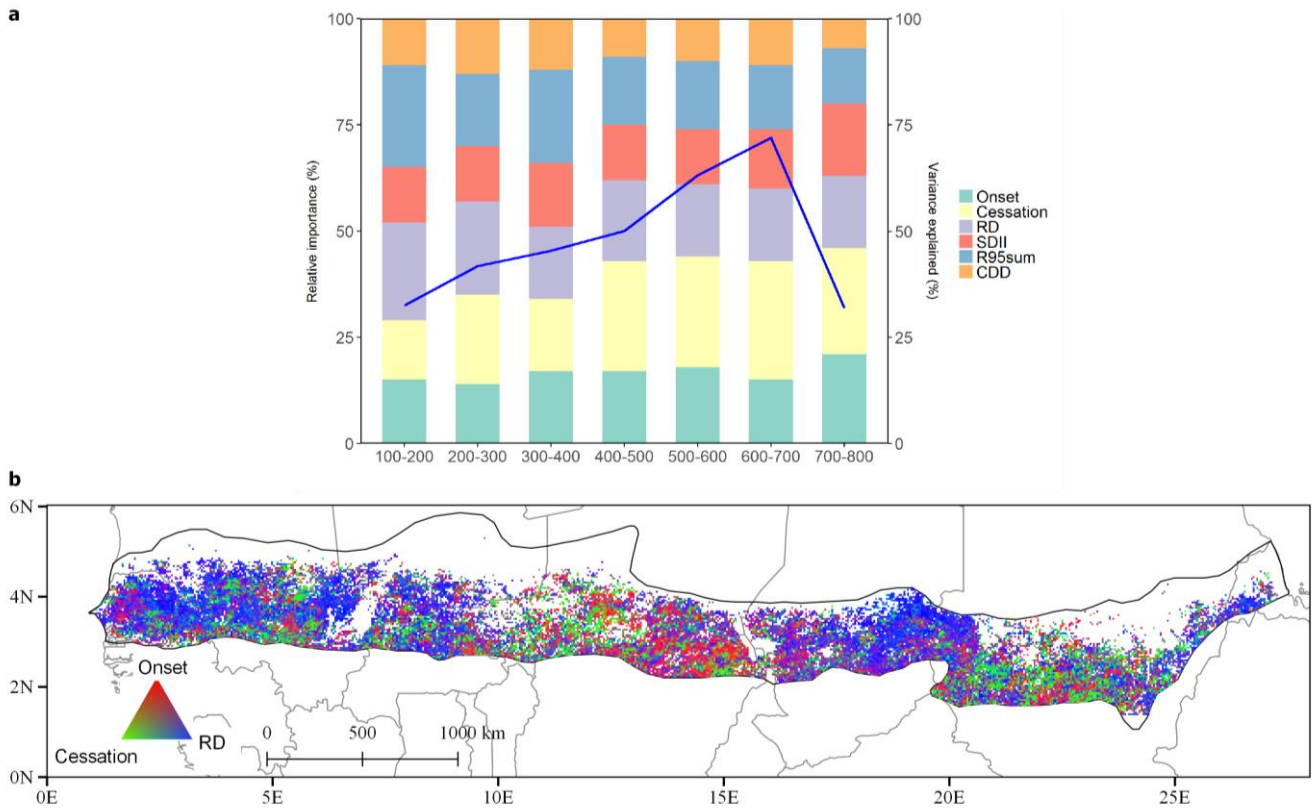


541

542 Fig.7. Effects of seasonal rainfall metrics on growing season ANPP as a function of seasonal rainfall amount. The non-
 543 parametric Spearman's rank correlation between growing season ANPP and rainfall metrics are shown for each 10 mm
 544 interval. The lines are GAM fitting curves and shading represents the 95% confidence intervals of the fitting.

545

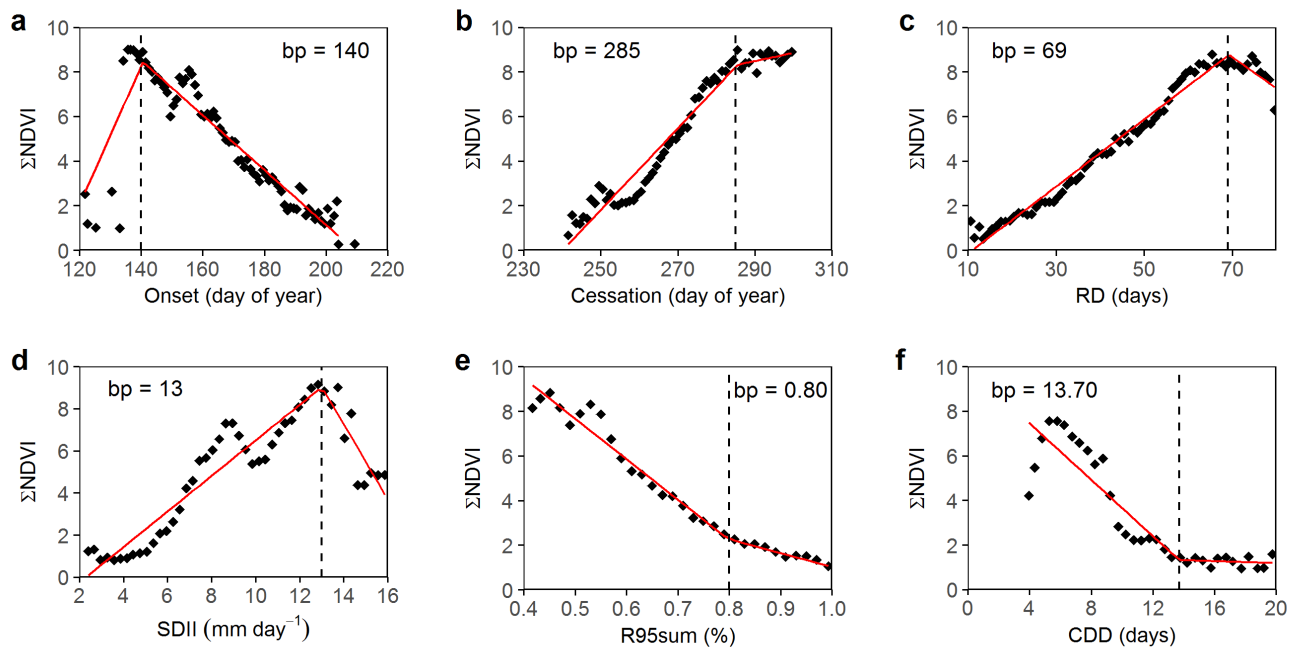
546



547

548 Fig.8. a) Generalized relationships between growing season ANPP and Onset, Cessation, RD, SDII, R95sum, CDD as a
 549 function of seasonal rainfall amount (100 mm intervals) based on 15-year average values (relative importance in %). The
 550 blue line shows the overall variance of growing season ANPP explained by the rainfall metrics per 100 mm seasonal rainfall
 551 amount based on the random forest method. b) Spatial distribution of the relative importance of onset, cessation of wet season
 552 and rainy days to growing season ANPP for 2001-2015 based on a multiple regression. Pixels within the study area are
 553 masked (white color) in accordance with the description in the methods section.

554



555

556 Fig. 9. Growing season ANPP (individual points represent 95th percentile of Σ NDVI value for each seasonal rainfall metric
 557 bins) plotted against rainfall metrics. Solid red lines denote piecewise regression between growing season ANPP and
 558 seasonal rainfall metrics and dashed lines indicate the breakpoint (bp) for rainfall individual metrics.

559